Separation Science and Technology
Publication details, including instructions for authors and subscription information:
http://www.informaworld.com/smpp/title~content=t713708471

Separation of benzene and cyclohexane mixtures using an NaY-type zeolite membrane

Byeong-Heon Jeong[a]; Yasuhisa Hasegawa[a]; Katsuki Kusakabe[a]; Shigeharu Morooka[a]
[a] Department of Applied Chemistry, Kyushu University, Fukuoka, Japan

To cite this Article Jeong, Byeong-Heon , Hasegawa, Yasuhisa , Kusakabe, Katsuki and Morooka, Shigeharu(2002) 'Separation of benzene and cyclohexane mixtures using an NaY-type zeolite membrane', Separation Science and Technology, 37: 6, 1225 — 1239

To link to this Article: DOI: 10.1081/SS-120002608

URL: http://dx.doi.org/10.1081/SS-120002608

SEPARATION SCIENCE AND TECHNOLOGY, 37(6), 1225–1239 (2002)

SEPARATION OF BENZENE AND CYCLOHEXANE MIXTURES USING AN NaY-TYPE ZEOLITE MEMBRANE

Byeong-Heon Jeong, Yasuhisa Hasegawa,
Katsuki Kusakabe, and Shigeharu Morooka*

Department of Applied Chemistry, Kyushu University,
Fukuoka 812-8581, Japan

ABSTRACT

An NaY-type zeolite membrane was formed on the outer surface of a 1.7-mm I.D. porous α-Al_2O_3 support tube using a hydrothermal synthesis. NaY-type zeolite powder was also prepared by the same procedure. The permeation and separation characteristics of single-component benzene (B) and cyclohexane (C), as well as an approximately equimolar mixture thereof, were investigated using the membrane at permeation temperatures of 358–413K. For the single-component systems, C permeated through the membrane faster than B, and the permeances to B and C increased with increase in permeation temperature in the ranges $(0.6-3.0) \times 10^{-7}$ and $(2.3-6.4) \times 10^{-7}\,\mathrm{mol\,m^{-2}\,sec^{-1}\,Pa^{-1}}$, respectively. When the mixture was fed, however, B permeated faster than C, and the separation factor was dependent on the partial pressures on both the feed and permeate sides. The B/C separation factor reached 107 at a permeation temperature of

---

*Corresponding author. Fax: 81-92-651-5606; E-mail: smorotcf@mbox.nc.kyushu-u.ac.jp

373K. The amounts of B and C, which were adsorbed to the NaY-type zeolite powder, were also determined at this temperature. The composition in the gas phase was maintained at approximately an equimolar ratio for the two components, and the total pressure of B and C was maintained at the pressures used for the permeation tests in the present study. The adsorption of B was approximately nine times that of C. Thus the B/C adsorption selectivity on the feed-side surface of the membrane was not the major factor for the high B/C separation factors.

Key Words: NaY-type zeolite; Membrane; Vapor permeation; Separation factor; Hydrocarbon vapor; Adsorption

INTRODUCTION

Benzene (B) and cyclohexane (C) are important starting materials of a variety of petrochemical products. Since the boiling points of these compounds are very close (353.2 and 353.9K, respectively), azeotropic distillation and extraction distillation are used frequently for their separation with the addition of a third component. This complexity increases the cost of these separation processes. Thus, it would be desirable to develop a process in which B and C can be separated directly. During the past decade, a number of polymer membranes have been developed and applied to the separation of B–C mixtures. As reviewed by Garvia Villaluenga and Tabe-Mohammade (1), separation factors, as well as permeation rates, of polymer membranes vary over a wide range, and the majority of polymeric membranes show B/C separation factors in the range 5–30. However, aromatic compounds with higher adsorptivities, when included in the feed, accumulate in the membrane. This accumulation causes the membrane to become swollen, and, as a result, can lead to a decrease in the separation factor. Thus, inorganic membranes, such as zeolite membranes, would be expected to be inherently superior for the separation of organic compounds.

Organic compounds with molecular sizes larger than the pores of zeolites, cannot permeate through the defect-free membranes. Organic compounds, which have a molecular size similar to the zeolitic channels, can permeate through the membranes by single-file diffusion mechanism, but cannot pass one another inside the pores. When a mixture of binary components is introduced into the feed side of a membrane, molecules with higher diffusivity are retarded greatly, and molecules with slower diffusivity are speeded up to some extent (2,3). Thus, the role of diffusivities, in predicting a separation factor for single file diffusion, is not large.

A number of studies have been reported on permeation through MFI-type zeolite membranes. The separation factor for binary mixtures is determined largely by adsorption selectivity on the feed-side surface of the membrane. The more strongly adsorbing component retards the adsorption of the less-adsorbing component. This effect increases the separation factor in preference of the strongly adsorbing component. However, the Maxwell–Stefan diffusivity of the strongly adsorbing component is usually smaller than that of the less-adsorbing component (4), which decreases the separation factor.

Krishna et al. (5,6) attempted to explain the permeation of a 1:1 mixture of *n*-hexane and 2,2-dimethylbutane, reported by Gump et al. (7), assuming that the Maxwell–Stefan diffusivities of these components were the same in the membrane. However, Noble et al. (7–15) reported that separation factors for hydrocarbons through MFI-type zeolite membranes were affected greatly by adsorption in nonzeolitic pores. Molecules permeate through nonzeolitic pores faster than through zeolitic pores. Thus, the overall separation factor can be strongly dependent on the pore size distribution in the membranes. Diffusion in the MFI-type zeolite has been discussed by many workers (16–20). However, the characterization of zeolitic and nonzeolitic pores in MFI-type zeolite membranes remains arbitrary.

Morooka and coworkers (21–24) have developed faujasite (FAU)-type zeolite membranes for use in gas separation. The FAU-type zeolite is composed of supercages, 1.1 nm in diameter, and interconnecting pores, 0.74 nm in diameter. This structure may lead to a selective permeation of hydrocarbon compounds, such as B and C, the molecular sizes of which are smaller than the interconnecting pores of the FAU-type zeolite. The molecules can pass one another in the cages of the FAU-type zeolite, and the limitation of the single-file diffusion can be avoided. Transport phenomena in the FAU-type zeolite have also been studied by Masuda et al. (25), Papaionnou et al. (26), and Fujikata et al. (2) and Sakuth et al. (27). Recently, Nikolakis et al. (28) prepared FAU-type zeolite membranes and separated B and C. The B/C separation factor was higher than 100 at 373K for an equimolar mixture under a total hydrocarbon pressure of 10 kPa. They attempted to explain the separation factor using adsorption isotherms in the literature (29) and assuming Maxwell–Stefan diffusivities. However, the relationship between selectivities for adsorption and permeation has not yet been clarified fully.

In the present study, an NaY-type zeolite membrane was prepared by hydrothermal synthesis. The permeation and separation characteristics for mixtures of B and C through the membranes were investigated by vapor permeation. The mechanism of separation for the binary mixture is discussed on the basis of adsorption properties.

EXPERIMENTAL

Preparation of the NaY-type Membrane

Porous α-Al_2O_3 tubes (NOK Corp., Japan, length = 200 mm, i.d. = 1.7 mm, o.d. = 2.1 mm, void fraction = 0.39, mean pore diameter = c.a. 150 nm) were used as the support for the zeolite membranes. The outer surface of the support tube, except for the central section, which was 13–15 mm length, was sealed with a glass sealant (Nippon Electric Glass Corp., GA-4). The area, wherein the gas permeation occurred, was $(7.7–8.9) \times 10^{-5}\,m^2$. The outer surface of the support tube was rubbed with NaY-type zeolite crystals (Tosoh Corp., #HSZ-320NAA, $Si/Al = 2.8$, crystal size = 0.5 μm) in order to implant seeds for nucleation. Both glass-coated end sections were wrapped with a polytetrafluorocarbon tape, in order to prevent the dissolution of the glass sealant. The support tube was then placed in a tubular autoclave, which was maintained in a horizontal position. The solution used for the synthesis was composed of water glass, sodium aluminate, and sodium hydroxide, dissolved in deionized water, and was stirred for 4 hr at ambient temperature. The initial composition was $Al_2O_3 : SiO_2 : Na_2O : H_2O = 1 : 12.8 : 17 : 975$ on a molar basis. The hydrothermal reaction was performed at 363K for 24 hr. During the synthesis, the autoclave was shaken at 2-hr intervals, in order to exchange the solution throughout the inside of the tube. The NaY-type zeolite membrane, which was formed on the outer surface of the support tube, was washed with deionized water and then dried in air for 12 hr. After the synthesis, the outer surface of the support tube, except for the permeating portion, was sealed with a polytetrafluorocarbon tube, which was gas-tightly shrunk by heat-treatment at 358K for 30 min. The heat-treatment was carried out at a heating and cooling rate of $1\,K\,min^{-1}$, in order to prevent the thermal destruction of the zeolite membrane. NaY powder was also prepared under the same conditions as were used for the synthesis of the zeolite membrane.

Adsorption Tests

Adsorption isotherms of single component B and C, as well as mixtures thereof, were determined for the NaY-type zeolite powder at 373K. The adsorption apparatus (BEL Japan, FMS-BG-H50) was equipped with a magnetically suspended thermobalance and precision pressure sensors, and could evaluate isotherms of two components. In order to increase the difference in the molar masses, deuterium-substituted C was used. The total adsorbed mass of B (molar mass $B_m = 0.078\,kg\,mol^{-1}$) and cyclohexane-$D_{12}$ (molar mass $C_m =$

$0.096\,\mathrm{kg\,mol^{-1}}$) is expressed by

$$M_t = M_B + M_C \tag{1}$$

The total pressures of B and C in the gas phase for the initial and equilibrated states, P_{0t} and P_t, respectively, are described as follows:

$$P_{0t} = p_{0B} + p_{0C} \tag{2}$$

$$P_t = p_B + p_C \tag{3}$$

The material balance after equilibration is

$$\frac{P_{0t}V}{RT} = \frac{P_tV}{RT} + \frac{M_B}{B_m} + \frac{M_C}{C_m} \tag{4}$$

The adsorbed mass of C is given by

$$M_C = \frac{[M_t/B_m - (P_{0t} - P_t)V/(RT)]}{(1/B_m - 1/C_m)} \tag{5}$$

The fraction of C in the gas phase after equilibration is derived as follows:

$$f_C = \frac{[f_{0C}P_{0t}V/(RT) - M_C/C_m]}{[P_tV/(RT)]} \tag{6}$$

The adsorbed mass and the gas phase fraction for B can be derived in a similar manner. The above equations are given to demonstrate the principle of the analysis. The actual apparatus contained two cells, which were used for storage of the feed mixture and for adsorption.

Vapor Permeation Tests

Permeation rates of the membrane were determined using single component B and C, as well as mixtures thereof, in the temperature range 358–413K. The vapor was diluted in a flow of nitrogen and introduced into the feed side. Nitrogen was also used as the sweep on the permeate side. Hydrocarbon concentrations were determined using a gas chromatograph equipped with a flame ionization detector (Shimadzu GC-8A). The partial pressure of each permeant was determined at the inlet and outlet on the feed and permeate sides, and a mean value on each side was calculated by logarithmically averaging the data. The flow rates were determined with soap–film flow meters. The total pressure on both sides was maintained at 101.3 kPa throughout the experiments. Permeance to component i, π_i, is defined in moles of the component per unit time and unit membrane area, divided by the partial pressure difference between the feed and permeate sides. The separation factor, $\alpha(\mathrm{B/C})$, is defined as the ratio of the permeances, i.e., π_B/π_C.

RESULTS

Adsorption

Figure 1 shows the adsorption isotherms for single-component B and C at 373K. For both components, the adsorption increased with increase in pressure. In the entire pressure range tested, the adsorption of B was higher than that of C. Table 1 shows the adsorbed amounts of B and C for the binary system at 373 K. At a total hydrocarbon pressure of 11.0 kPa, the adsorption of B was approximately nine times that of C. The total amount of adsorbed B and C was in the middle of the values for the single-component systems, shown in Fig. 1.

Permeation

The NaY-type zeolite membrane, which was formed on the outside of the support, consisted of two zeolite layers, an inner layer formed in the voids of the support (ca. 5 μm in thickness) and an outer layer formed on the support (ca. 3 μm in thickness). No crystal growth was observed on the inside of the support.

Figure 2 shows the permeances to B and C for the single-component systems at a permeation temperature of 373K. The partial pressure on the feed side was 7.6 kPa for B and 8.5 kPa for C. The sweep flow rate was maintained at 10 ccm (cm^3(STP) per minute), and the partial pressure on the permeate side, 0.25 kPa for B and 0.76 kPa for C, was much lower than the partial pressure on the feed side. As described below, the permeances are dependent on the partial pressures on the permeate side, and are therefore shown in the figure. The permeance reached a steady-state value soon after the start of permeation for both components.

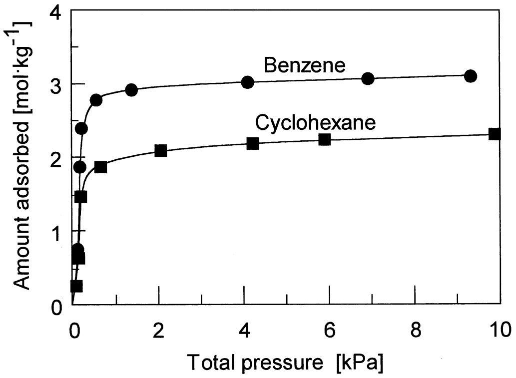

Figure 1. Amount adsorbed on Y-type zeolite for single-component systems at 373K.

Table 1. Amounts Adsorbed for the Binary System at 373K

System	Partial Pressure (kPa)	Amount Adsorbed	Adsorption Selectivity
Benzene/cyclohexane	5.4/5.6	2.41/0.26	9

Figure 3 shows the effect of permeation temperature on the permeances for single-component systems. The partial pressure on the feed side was 7.6 kPa for B and 8.5 kPa for C, and the sweep flow rate on the permeate side was 10 ccm. The partial pressures on the permeate side were much lower than the partial pressures on the feed side. The permeances to B and C increased with increase in temperature, indicating that an activated transport mechanism was operational. At all the tested permeation temperatures for the single-component systems, the permeance to C was higher than that to B. The separation factor, $\alpha(B/C)$, increased and approached unity with an increase in permeation temperature.

At a permeation temperature of 373K, C was fed continuously to the feed side at $p_{fC} = 5.98$ kPa, and B was then introduced at $p_{fB} = 4.92$ kPa, as shown in Fig. 4. After an operation period of 25 hr, the flow of B was stopped, and a single flow of C was restored. During the feed of the mixture, p_{fC} was 3.67 kPa, which was somewhat lower than the initial value. The C flux was decreased sharply, immediately after the introduction of B, and returned to the initial value after the B feed was terminated. The finding that the permeance to B was higher than that

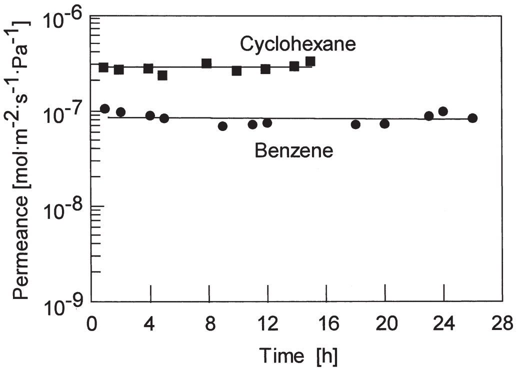

Figure 2. Permeances to single-component B and C at 373K. $p_{fB} = 7.6$ kPa, $p_{fC} = 8.5$ kPa, $p_{pB} = 0.25$ kPa, $p_{pC} = 0.76$ kPa.

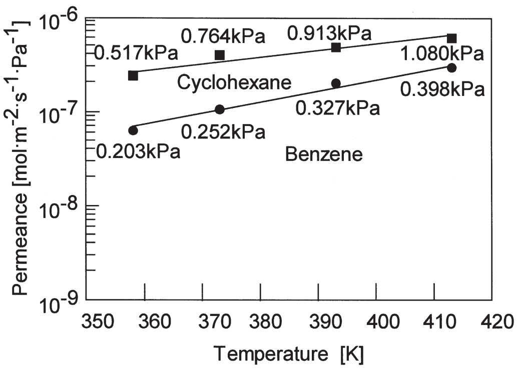

Figure 3. Effect of permeation temperature on permeances to single-component B and C. $p_{fB} = 7.6\,\text{kPa}$, $p_{fC} = 8.5\,\text{kPa}$.

to C is contrary to the result for single-component systems, where the separation factor, $\alpha(B/C)$, was determined to be 0.2–0.6.

Figure 5 shows the effect of permeation temperature on the permeances to B and C. The partial pressure on the feed side was 5.1 kPa for B and 4.0 kPa for C. The sweep flow rate was 10 ccm and the partial pressures of the organic components were as shown in the figure. The trend for the permeances to increase with the increasing permeation temperature was the same as for the single-component systems, but the permeance to B was larger than that to C. The separation factor, $\alpha(B/C)$, was the largest at 373K, as shown in Fig. 6.

The permeances for the binary mixture under partial pressures on the feed side, $p_{fB} = 5.1\,\text{kPa}$ and $p_{fC} = 4.0\,\text{kPa}$, was also dependent on the flow rate of the sweep. Figure 7 shows the permeances to B and C through the membrane as a function of the sweep gas flow rate (10–100 ccm) at 373K. The permeance to B increased, and that to C decreased, with a decrease in the partial pressure of each permeant on the permeate side. This suggests that the adsorbed amounts of the permeants, irrespective of their small values, affect the permeation rate. The highest separation factor of 107 was obtained when the sweep gas flow rate was 100 ccm.

DISCUSSION

Krishna and coworkers (5,6,17) analyzed the effect of adsorption on separation factors for multicomponent systems in MFI-type zeolite membranes. For binary mixtures, the diffusion of component i ($i = 1, 2$) in the membrane can

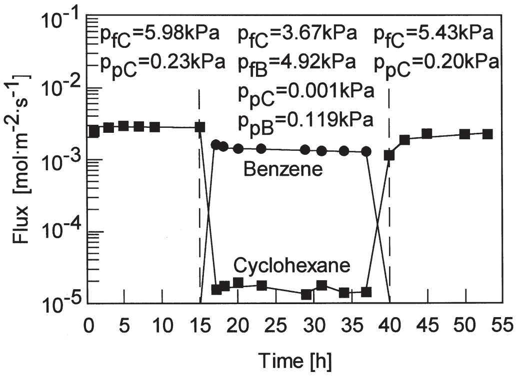

Figure 4. Changes in permeation fluxes for single- and binary-component systems at 373K.

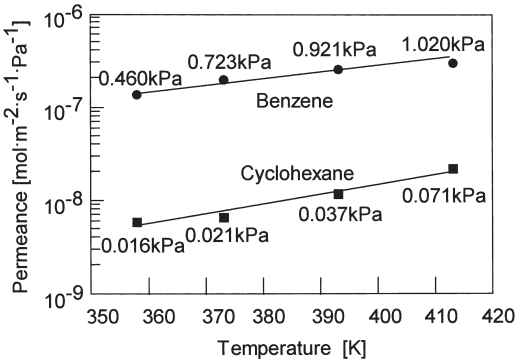

Figure 5. Effect of permeation temperature on permeances for a binary system of B and C. $p_{\mathrm{fB}} = 5.1\,\mathrm{kPa}$, $p_{\mathrm{fC}} = 4.0\,\mathrm{kPa}$.

be described as

$$N_i = -\frac{\rho \Theta_{i,\mathrm{sat}} D_{i,\mathrm{eff}} \mathrm{d}\theta_i}{\mathrm{d}z} \tag{7}$$

$$\begin{vmatrix} D_{1,\mathrm{eff}} \\ D_{2,\mathrm{eff}} \end{vmatrix} = \begin{vmatrix} 1/\boldsymbol{D}_1 + \theta_2/\boldsymbol{D}_{12} & -\theta_1/\boldsymbol{D}_{12} \\ -\theta_2/\boldsymbol{D}_{12} & 1/\boldsymbol{D}_2 + \theta_1/\boldsymbol{D}_{12} \end{vmatrix}^{-1} + \begin{vmatrix} \Gamma_{11} & \Gamma_{12} \\ \Gamma_{21} & \Gamma_{22} \end{vmatrix} \tag{8}$$

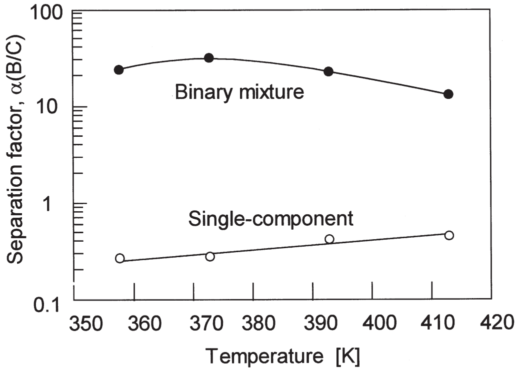

Figure 6. Effect of permeation temperature on separation factor. Conditions are the same as shown in Figs. 3 and 5.

The thermodynamic correction factor is given by

$$\Gamma_{ij} = \left(\frac{\theta_i}{p_i}\right)\left(\frac{\partial p_i}{\partial \theta_j}\right) \quad i,j = 1,2 \tag{9}$$

The effective Fick diffusivities are given by

$$D_{1,\mathrm{eff}} = D_1 \pm D_{12}\left|\frac{\nabla\theta_2}{\nabla\theta_1}\right| \tag{10}$$

$$D_{2,\mathrm{eff}} = \pm D_{12}\left|\frac{\nabla\theta_1}{\nabla\theta_2}\right| + D_2 \tag{11}$$

Krishna and Paschek (6) assumed positive signs on the right-hand side of Eqs. (10) and (11), and analyzed the permeation rates through MFI-type zeolite membranes for combinations of C_6 hydrocarbons, as reported by Noble and coworkers (10,11,13). Since the effective diffusivity of the less adsorptive component is higher than that of the more adsorptive component, the permeation separation factor is smaller than the selectivity for adsorption. However, the separation factors for permeation, α(*n*-hexane/DMB), reported by Flanders et al. (13), exceeded 1000 at 350–400K, and were much higher than the adsorption selectivities estimated by Krishna and Paschek (6).

As shown in Fig. 4, the separation factor, $\alpha(\mathrm{B/C})$, was reversed completely for the single-component and binary systems. This result is in agreement with that of Nikolakis et al. (28), who used the same combination of membranes and permeates as were used in the present study. The reversal of separation factors for

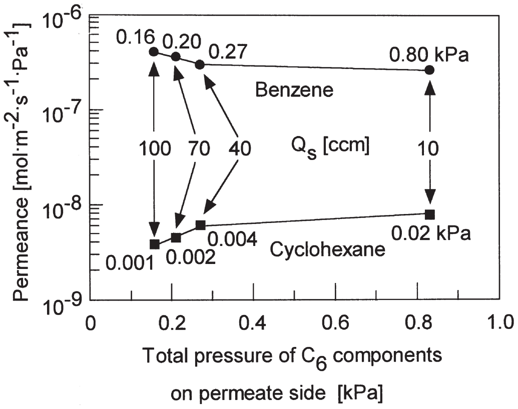

Figure 7. Effect of hydrocarbon pressures on permeances for a binary system of B and C at 373K. $p_{\mathrm{fB}} = 5.1\,\mathrm{kPa}$, $p_{\mathrm{fC}} = 4.0\,\mathrm{kPa}$, Q_s = sweep flow rate.

the single- and binary-component systems was also reported by Funke et al. (8), using MFI-type zeolite membranes for combinations of *n*-octane, *iso*-octane, and *n*-hexane. For single-component systems, the permeance was in the order of *n*-hexane > *iso*-octane > *n*-octane. For a ternary system, the permeance was in the order of *n*-octane > *iso*-octane > *n*-hexane. The presence of *n*-hexane increased greatly the permeance to *n*-octane. However, Funke et al. (10) did not observe the reversal of separation factors for combinations of alkanes and B, alkanes and toluene, as well as *n*-hexane and C.

Nikolakis et al. (28) applied the Maxwell–Stefan formulation to the permeation of a B–C mixture through the X-type membrane.

$$N_i = cD_{i,\mathrm{eff}}\Theta_{i,\mathrm{sat}}b_i(p_{\mathrm{f}i} - p_{\mathrm{p}i}) \tag{12}$$

where c is a constant which is common to all permeants, and $\Theta_{i,\mathrm{sat}}b_ip_{\mathrm{f}i}$ is the amount adsorbed on the feed-side surface of the membrane. If the effective diffusivity of B is smaller than that of C, the high separation factors must be attributed to high B/C adsorption selectivities. Nikolakis et al. (28) assumed these types of isotherms from the data for single-component systems (29). As shown in Table 1, however, the B/C adsorption selectivities are not high at the partial pressures of 3–5 kPa, used in the study of Nikolakis et al. (28), as well as in the present work. As a result, the separation factor, $\alpha(\mathrm{B/C})$, exceeds greatly the adsorption selectivity on the feed-side surface of the membrane. The negative signs in the right-hand side of Eqs. (10) and (11) could be important for estimating diffusivities for binary systems, as claimed by Sundaram and Yang (30).

CONCLUSIONS

An NaY-type zeolite membrane was formed on the outer surface of a porous α-Al_2O_3 support tube. The permeation and separation characteristics of single component B and C, as well as mixtures thereof, through the membrane were investigated. The permeation temperature was varied in the range of 358–413K. For the case of single-component systems, C permeated faster than B. For a mixed feed, however, B permeated through the membrane faster than C. The separation factor, $\alpha(B/C)$, was dependent on the permeation temperature and the partial pressures of the gas phase on the feed and permeate sides. The highest separation factor was 107 at 373K. The adsorption data showed that this separation factor was much higher than the value calculated from the adsorption selectivity on the feed-side surface of the membrane. This suggests that the effective diffusivity of C in the Y-type zeolite membrane could be much smaller than that of B. A further study on the adsorption characteristics for binary systems is now under way.

NOTATION

$\boldsymbol{D}_i$	Maxwell–Stefan diffusivity of component *i*
$\boldsymbol{D}_{ij}$	Maxwell–Stefan interchange diffusivity for combination of *i* and *j*
$D_{i,\mathrm{eff}}$	effective diffusivity of component *i*
D_i	Fick diffusivity of component *i*
D_{ij}	Fick interchange diffusivity for combination of *i* and *j*
f_i	final mole fraction of component *i* in the gas phase for adsorption test
F_{0i}	initial mole fraction of component *i* in the gas phase for adsorption test
M_i	mass of adsorbed *i* component for adsorption test
M_t	mass of total adsorbed hydrocarbons for adsorption test
N_i	flux of component *i*
P_t	final total hydrocarbon pressure
$P_{0\mathrm{t}}$	initial total hydrocarbon pressure for adsorption test
p_i	final partial pressure of component *i* for adsorption test
p_{0i}	initial partial pressure of component *i* for adsorption test
$p_{\mathrm{f}i}$	partial pressure of component *i* on the feed side
$p_{\mathrm{p}i}$	partial pressure of component *i* on the permeate side
R	gas constant
T	temperature
V	total volume of the adsorption unit

z	distance from the feed-side surface of the membrane
$\alpha(i/j)$	separation factor of component i to component j
Γ_{ij}	thermodynamic correction factor for combination of i and j
$\Theta_{i,\mathrm{sat}}$	adsorbed amount of component i at saturation
θ_i	fractional surface occupancy of component i
π_i	permeance of component i
ρ	density of zeolite

Subscripts

B	Benzene
C	Cyclohexane

ACKNOWLEDGMENTS

This work was supported by the Japan Society for the Promotion of Science (JSPS), as well as the New Energy and Industrial Technology Development Organization (NEDO) of Japan. We also acknowledge sincerely the useful discussion with Professor T. Masuda, Kyoto University, and Professor K. Chihara, Meiji University, and the support of NOK Corporation, Japan.

REFERENCES

1. Garcia Villaluenga, J.P.; Tabe-Mohammadi, A. A Review on the Separation of Benzene/Cyclohexane Mixtures by Pervaporization Processes. J. Membr. Sci. **2000**, *169*, 159–174.
2. Fujikata, Y.; Masuda, T.; Ikeda, H.; Hashimoto, K. Measurement of the Diffusivities Within MFI- and Y-Type Zeolite Catalysts in Adsorption and Desorption Processes. Microporous Mesoporous Mater. **1998**, *21*, 679–686.
3. Masuda, T.; Fujikata, Y.; Ikeda, H.; Hashimoto, K. Diffusivities in the Binary Component System Within MFI-Type Zeolite Crystals. Microporous Mesoporous Mater. **2000**, *38*, 323–332.
4. van de Graaf, J.M.; Kapteijn, F.; Moulijn, J.A. Diffusivities of Light Alkanes in a Silicalite-1 Membrane Layer. Microporous Mesoporous Mater. **2000**, *35-36*, 267–281.
5. Krishna, R.; Vlugt, T.J.H.; Smit, B. Influence of Isotherm Inflection on Diffusion in Silicalite. Chem. Eng. Sci. **1999**, *54*, 1751–1757.
6. Krishna, R.; Paschek, D. Separation of Hydrocarbon Mixtures Using Zeolite Membranes: A Modelling Approach Combining Molecular

Simulations with the Maxwell–Stefan Theory. Sep. Purif. Technol. **2000**, *21*, 111–136.

7. Gump, C.J.; Noble, R.D.; Falconer, J.L. Separation of Hexane Isomers Through Nonzeolite Pores in ZSM-5 Zeolite Membranes. Ind. Eng. Chem. Res. **1999**, *38*, 2775–2781.
8. Funke, H.H.; Kovalchick, M.G.; Falconer, J.F.; Noble, R.D. Separation of Hydrocarbon Isomer Vapors with Silicalite Zeolite Membranes. Ind. Eng. Res. **1996**, *35*, 1575–1582.
9. Funke, H.H.; Argo, A.M.; Baertsch, C.D.; Falconer, J.F.; Noble, R.D. Separation of Close-Boiling Hydrocarbons with Silicalite Zeolite Membranes. J. Chem. Soc. Faraday Trans. **1996**, *92*, 2499–2502.
10. Funke, H.H.; Argo, A.M.; Falconer, J.F.; Noble, R.D. Separation of Cyclic, Branched, and Linear Hydrocarbon Mixtures Through Silicalite Membranes. Ind. Eng. Chem. Res. **1997**, *36*, 137–143.
11. Baertsch, C.D.; Funke, H.H.; Falconer, J.L.; Noble, R.D. Permeation of Aromatic Hydrocarbon Vapors Through Silicalite–Zeolite Membranes. J. Phys. Chem. **1996**, *100*, 7676–7679.
12. Gump, C.J.; Lin, X.; Falconer, J.L.; Noble, R.D. Experimental Configuration and Adsorption Effects on the Permeation of C4 Isomers Through ZSM-5 Zeolite Membranes. J. Membr. Sci. **2000**, *173*, 35–52.
13. Flanders, C.L.; Tuan, V.A.; Noble, R.D.; Falconer, J.L. Separation of C_6 Isomers by Vapor Permeation and Pervaporation Through ZSM-5 Membranes. J. Membr. Sci. **2000**, *176*, 43–53.
14. Tuan, V.A.; Falconer, J.L.; Noble, R.D. Isomorphous Substitution of Al, Fe, B, and Ge into MFI-Zeolite Membranes. Microporous Mesoporous Mater. **2000**, *41*, 269–280.
15. Tuan, V.A.; Noble, R.D.; Falconer, J.L. Boron-Substituted ZSM-5 Membranes: Preparation and Separation Performances. Am. Inst. Chem. Eng. J. **2000**, *46*, 1201–1208.
16. Wegner, K.; Dong, J.; Lin, Y.S. Polycrystalline MFI-Zeolite Membranes: Xylene Pervaporation and Its Implication on Membrane Microstructure. J. Membr. Sci. **1999**, *158*, 17–27.
17. Kapteijn, F.; Moulijn, J.A.; Krishna, R. The Generalized Maxwell–Stefan Model for Diffusion in Zeolites: Sorbate Molecules with Different Saturation Loadings. Chem. Eng. Sci. **2000**, *55*, 2923–2930.
18. Matsufuji, T.; Nishiyama, N.; Matsukata, M.; Ueyama, K. Separation of Butane and Xylene Isomers with MFI-Type Zeolite Membrane Synthesized by a Vapor-Phase Transport Method. J. Membr. Sci. **2000**, *178*, 25–34.
19. Matsufuji, T.; Watanabe, K.; Nishiyama, N.; Egashira, Y.; Matsukata, M.; Ueyama, K. Permeation of Hexane Isomers Through an MFI Membrane. Ind. Eng. Chem. Res. **2000**, *39*, 2434–2438.

20. Xomeritakis, G.; Nair, S.; Tsapatsis, M. Transport Properties of Alumina-Supported MFI Membranes Made by Secondary (Seeded) Growth. Microporous Mesoporous Mater. **2000**, *38*, 61–73.
21. Kusakabe, K.; Kuroda, T.; Morooka, S. Separation of Carbon Dioxide from Nitrogen Using Ion-Exchanged Faujasite-Type Zeolite Membranes Formed on Porous Support Tubes. J. Membr. Sci. **1998**, *148*, 13–23.
22. Kusakabe, K.; Kuroda, T.; Uchino, K.; Hasegawa, Y.; Morooka, S. Gas Permeation Properties of Ion-Exchanged Faujasite-Type Zeolite Membranes. Am. Inst. Chem. Eng. J. **1999**, *45*, 1220–1226.
23. Hasegawa, Y.; Watanabe, K.; Kusakabe, K.; Morooka, S. The Separation of CO_2 Using Y-Type Zeolite Membranes Ion-Exchanged with Alkali Metal Cations. Sep. Purif. Technol. **2001**, *22–23*, 319–325.
24. Hasegawa, Y.; Kusakabe, K.; Morooka, S. Effect of Temperature on the Gas Permeation Properties of NaY-Type Zeolite Formed on the Inner Surface of a Porous Support Tube. Chem. Eng. Sci. **2001**, *56*, 4273–4281.
25. Masuda, T.; Fukuda, K.; Fujikata, Y.; Ikeda, H.; Hashimoto, K. Measurement and Prediction of the Diffusivity of Y-Type Zeolite. Chem. Eng. Sci. **1996**, *51*, 1879–1888.
26. Papaioannou, C.; Petroutsos, G.; Gunßer, W. Examination of the Adsorption of Hydrocarbons at Low Coverage on Faujasite Zeolites. Solid State Ionics **1997**, *101–103*, 799–805.
27. Sakuth, M.; Meyer, J.; Gmehling, J. Measurement and Prediction of Binary Adsorption Equilibria of Vapors on Dealuminated Y-Zeolites (DAY). Chem. Eng. Process. **1998**, *37*, 267–277.
28. Nikolakis, V.; Xomeritakis, G.; Abibi, A.; Dickson, M.; Tsapatsis, M.; Vlachos, D.G. Growth of a Faujasite-Type Zeolite Membrane and Its Application in the Separation of Saturated/Unsaturated Hydrocarbon Mixtures. J. Membr. Sci. **2001**, *184*, 209–219.
29. Ruthven, D.M.; Doetsch, I.H. Diffusion of Hydrocarbons in 13X Zeolite. Am. Inst. Chem. Eng. J. **1976**, *22*, 882–886.
30. Sundaram, N.; Yang, R.T. Binary Diffusion of Unequal Sized Molecules in Zeolites. Chem. Eng. Sci. **2000**, *55*, 1747–1754.

Received April 2001
Revised August 2001